QATAR UNIVERSITY

COLLEGE OF ARTS AND SCIENCES

RELATIONSHIP BETWEEN STRUCTURE, PROPERTIES AND UV/HEAT PROTECTION BEHAVIOUR OF TWO DIFFERENT TYPES OF POLYETHYLENE MANUFACTURED IN QATAR

BY

SOUMIA GASMI

A Project Submitted to

the Faculty of the College of Arts and Sciences

in Partial Fulfillment of the Requirements for the Degree of

Masters of Science in Material Science and Technology

January 2021

COMMITTEE PAGE

The members of the Committee approve the Project of

SOUMIA GASMI defended on 06/12/2020.

_____

Dr. Igor Krupa

Thesis/Dissertation Supervisor

_____

Dr. Aboubakr M. Abdullah Ali

Committee Member

_____

Prof. Talal Altahtamouni

Committee Member

ABSTRACT

GASMI, SOUMIA, A., Masters : January : [2021:], Material Science and Technology

Title: Relationship between Structure, Properties and UV/heat Protection Behaviour of Two Different Types of Polyethylene Manufactured in Qatar

Supervisors of Project: Dr. Igor Krupa and Prof. Adriaan S. Luyt.

Accelerated (artificial) weathering and thermal ageing tests were performed to investigate the effectiveness of different UV/HALS formulations in reducing the UV/heat degradation effect for two different low-density polyethylene grades with different structures because of production through two different production methods (autoclave and tubular reactors). Combinations of two commercial-grade HALS (Chimassorb 944 and Sabostab 119) and two UV absorbers (Chimasorb 81 and Tinuvin 1577) were introduced to both the LDPE grades at different loadings. The morphologies, as well as thermal and mechanical properties, of the investigated samples were determined through tensile and impact testing, gel permeation chromatography (GPC), scanning electron microscopy (SEM), Fourier-transform infrared (FTIR) spectroscopy, differential scanning calorimetry (DSC), and thermogravimetric analysis (TGA). All the results from the different characterization techniques showed a significant degradation for the unstabilized neat samples of both LDPEs, while little or no degradation was observed for the stabilized ones, confirming the effectiveness of the selected UV/HALS systems in improving the weathering resistance of the two LDPE grades and enhancing their useful lifetime. The GPC results showed that the LDPE-A contained significantly more long-chain branching (LCB) than the LDPE-T, implying that the LDPE-A was much more compact than the LDPE-T. Young's modulus values for LDPE-T

were much higher than those of LDPE-A, indicating a higher crystallinity of the LDPE-T samples. For the heat exposed samples, more brittle behaviour was observed for the LDPE-T samples. There was very little difference in the maximum tensile stress values of LDPE-A and LDPE-T, except for LDPE-T/UV3 where the σ_{value} increased by about 9% after 12 months. LDPE-T was found to be thermally more stable than LDPE-A, even after long UV exposure times. For stabilized formulations, LDPE-A/UV8 seems to be the best formulation in terms of thermal stability whereas LDPE-T/UV8 was the least promising formulation. Generally, the UV/heat stabilized LDPE-A samples were thermally more stable than LDPE-T The carbonyl indices were similar for the two polymers, which means that the differences in polymer structure had little influence on the formation of carbonyl groups during the oxidative degradation process.

DEDICATION

I dedicate this work to my parents and siblings; whose love and support knew no bounds.

To my amazing friends, who were the comforting sunshine in my hardest hours.

ACKNOWLEDGMENTS

First and foremost, I want to sincerely thank my supervisor, Prof. Adriaan, for all his help and guidance that have allowed me to finish this piece of work and grow as a person and a researcher.

I dearly send the warmest thank you to my dear friends and colleagues, Eng. Reem Al-Jindi and Eng. Sara Shahid, for their support, guidance and fruitful companionship to me during my project.

Finally, I would like the acknowledge the role of Qatar National Research Fund (a member of Qatar Foundation) in financially supporting this study through the National Priorities Research Program NPRP9-161-1-030.

TABLE OF CONTENTS

LIST OF TABLES

LIST OF FIGURES

LIST OF SUPPLEMENTARY TABLES

LIST OF SUPPLEMENTARY FIGURES

Chapter 1: Introduction

With the excessive use of polyolefins in domestic and industrial sectors, polyolefins, specifically polyethylenes (PEs), have received substantial attention and became a fundamental topic of research. Their demand has been reported to increase globally with an estimated annual production of 24 million tonnes [1]. Due to their unique and outstanding properties such as their toughness and flexibility, even at low temperatures, excellent chemical resistance, easy processability, freedom from odour and toxicity, and their low cost [2], polyethylenes have been widely used for numerous applications such as packaging, buildings, electrical fittings, and agricultural piping [2]. However, PEs like all organic materials suffer from poor weathering resistance under the influence of the different environmental factors such as heat, moisture, solar radiation, weather pollutants, and ultraviolet radiation [3], leading to an inevitable degradation which limits their service lifetime and severely restricts their performance for the outdoors applications [4].

Photodegradation of polymers is a combination of the oxidative effect of atmospheric oxygen with the photochemical and photophysical effects of ultraviolet radiation photons. The combined effect of oxygen and light radiation induces a complex set of processes that can cause undesirable changes on the appearance of the polymer's surface, such as discoloration, embrittlement, tackiness, loss of surface gloss, and crazing or chalking of the surface [5]. Due to the low diffusion coefficient of oxygen in most polymers, degradation is generally more sever at the outer surface of the polymer than in its bulk [5].

The development of highly effective and environmentally friendly UV stabilizing systems is crucial in the polyethylene industry. Antioxidants, UV absorbers,

and free radical scavengers are the most commonly used additives in the plastics industry. They are added to polymers designed purposely for outdoor applications to protect them from the synergistic effect of UV radiation and oxygen, as well as to improve their mechanical, processability, and miscibility behaviour. Antioxidants are chemical compounds that are commonly added to the polymer to protect it from the thermal and photooxidative processes caused by the various environmental factors during their outdoor natural ageing [6]. For example, phosphites (or phosphonites), secondary antioxidants, are extremely effective 'green' stabilizers during processing. Their role is simply to decompose peroxides and hydroperoxides resulting from the photooxidation process into stable, nonradical products [6]. UV absorbers, one the commonly used photostabilizers, protect the polymer from photo-oxidation by absorbing the harmful UV radiation (300-400 nm) during the first step of the photo-oxidation process, and preventing its interaction with the photoactive chromophoric species in the polymer molecule [6]. Hindered amine light stabilizers (HALS), that are long-term thermal stabilizers, have the ability to scavenge radicals created by UV absorption during the photo-oxidation processes by forming nitroxyl radicals through a cyclic mechanism known as the Denisov Cycle, and hence restricting the photodegradation process [6]. HALS are considered as one of the best and most efficient groups of UV stabilizers for most polyolefins, and they all share the 2,2,6,6-tetramethylpiperidine ring structure [6].

Tubular and autoclave reactor technologies are employed nowadays in the production of low-density polyethylene (LDPE) at high pressures and temperatures in the presence of specific chemical initiators *via* free radical reaction mechanisms [7]. In this work, the overall performance of diffferent UV formulations was compared for two different polyethylenes produced using different technologies; LDPE-A was

manufactured in an autoclave (batch process) and LDPE-T in a tubular reactor (continuous process). The main differences between the two polyethylene grades are the level and type of long-chain branching, as well as their molecular shape (Figure 1) [8,9]. LDPE-A is produced at constant temperature in well-stirred autoclave vessels under practically ideal mixing and presents broad molecular weight distributions with a bias towards the low molecular weight ends [8,9]. They are characterized by a simple structure of long chain branching, a globular molecular shape, tree-like branching, and low tensile strength. LDPE-T, produced in a very long and small diameter tubular reactor through a continuous tubular process [2], shows a narrower molecular weight distribution with a bias towards the high molecular weight end. LDPE-T displays a higher degree of long chain branching, and it is characterized by a linear molecular shape, comb-like branching and a high tensile strength [8-10].

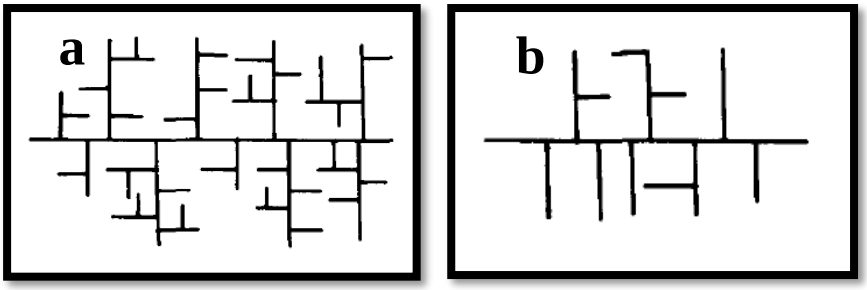

Figure 1. (a) Autoclave produced LDPE (LDPE-A) and (b) tubular reactor produced LDPE (LDPE-T).

Polymer weathering for combinations of different polyolefins with different HALS through natural (outdoor) or accelerated (artificial) modes have been performed and reported in different studies [11-15,19]. The synergistic and antagonistic effect of HALS and UV absorbers for stabilizing LDPE films was examined [11], where films containing a combination of HALS and UV absorbers reached 50% tensile strength retention within 590 days, whereas films containing a single HALS reached 50% tensile strength retention within only 205 days. The UV stability of the LDPE films was significantly improved by combining a HALS (Tinuvin 1577) with a UV absorber (Chimassorb 2020) [14]. The high molecular weight HALS was found to be effective for polyolefins not only as a UV stabilizer, but also as a long-term thermal stabilizer [13,16-19]. Several studies proved that HALS-3 or Chimassorb 944 is efficient as a UV and thermal stabilizer for LLDPE and LDPE films [13,17,19]. It was reported that Chimassorb 944 was successful in reducing the carbonyl index, which is considered as one of the main indicators of photodegradation [56]. The efficiency of HALS as a free radical scavenger during photo-oxidation processes was also studied and reported through multiple weathering studies [11,13,19].

Most published weathering studies examined the UV and thermal stability of one PE type and grade. However, in this study, we compared the effectiveness of different UV/HALS formulations in two different LDPEs with different structures as a result of different production methods, something we could not find in any previously published literature. We prepared the same UV absorber (Chimasorb 81 and Tinuvin 1577) and commercial grade HALS (Chimassorb 944 and Sabostab 119) combination formulations for both LDPEs, and we exposed samples of these formulations to accelerated weathering in a commercial weatherometer. The morphologies, as well as thermal and mechanical properties, of the investigated samples was determined

through tensile and impact testing, gel permeation chromatography (GPC), scanning electron microscopy (SEM), Fourier transform infrared (FTIR) spectroscopy, differential scanning calorimetry (DSC), and thermogravimetric analysis (TGA).

Chapter 2: Materials and Methods

2.1 Materials

Two commercial low-density polyethylene (LDPE) grades (LDPE-A and LDPE-T) were provided by Qatar Petrochemical Company (QAPCO, Doha, Qatar). LDPE-A (density = 920 kg m^{-3}, MFI = 0.3 g/10 min) refers to an LDPE manufactured in an autoclave (batch process) and LDPE-T (density = 923 kg m^{-3}, MFI = 0.3 g/10 min) to an LDPE manufactured in a tubular reactor (continuous process). Both polymers were received as pellets and powderized by Weaver Trading Company in South Africa.

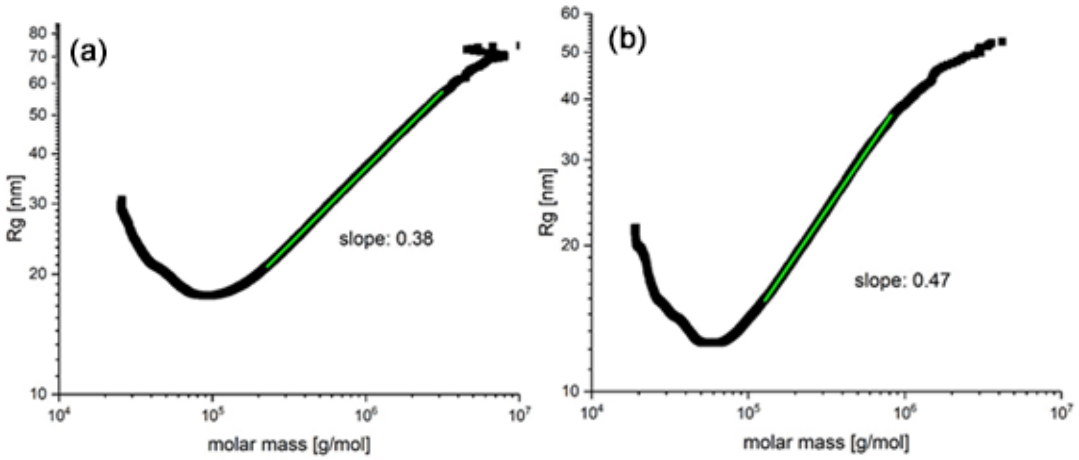

Figure 2. Conformation plot for (a) LDPE-A and (b) LDPE-T. The green line is a linear fit of the data.

The weight average molar masses and dispersities of the samples were characterized by gel permeation chromatography with multi angle laser light scattering (HT-GPC-MALS) and found to be M_w = 334.4 kg/mol / Đ = 4.4 (LDPE-A) and M_w = 155.1 kg/mol / Đ = 2.8 (LDPE-T). Their long-chain branching (LCB) content was similarly characterized and LDPE-A was found to contain significantly more LCB than LDPE-T. This is evident from the plots of the radius of gyration (Rg) of the samples as a function of molar mass (conformation plots) shown in Figure 2. The conformation plot for a linear polymer shows a slope of about 0.57, and with increasing LCB content smaller slopes are found as the molecules become more compact. LDPE-A is therefore much more compact than LDPE-T.

Chimassorb 944, Chimassorb 81, and Tinuvin 1577 were all supplied by BASF as HALS and UV absorbers. Sabostab 119 was supplied by Sabo as a HALS. Calcium stearate was supplied by Scientific Global Lab Supplies W.L.L.

2.2 Sample preparation

The formulations were prepared through thorough 20 min. bag-mixing of the specified amounts of powdered LDPEs and the selected additives. Table 1 summarizes the compositions used in preparing the UV protection formulations for LDPE-A and LDPE-T. 0.05 wt.% calcium stearate was added to all the formulations.

Table 1. Compositions of UV formulations in wt.%. All the formulations contained 0.05 wt.% calcium stearate.

LDPE		Chimassorb 81	Chimassorb 944	Sabostab 119	Tinuvin 1577
		UV absorber	HALS	HALS	UV absorber
UV3	99.75	0.1	0.1		
UV8	99.75			0.1	0.1

A twin-screw extruder KETSE 20/40 EC (Model no. 838106) was used to melt extrude the polymer/additive powder mixtures at a speed of 90 rpm and across a temperature range of 170-195 °C from feeder to die. The extruded mixture was then pelletized to ensure a smooth injection molding process. Impact and tensile specimens were prepared by injection molding using an ARBURG All-Rounder 570 C injection molding machine, across a 180-215 °C temperature range. The impact testing samples were produced with dimensions of 63.5 mm long x 12.7 mm wide x 3 mm thick (ASTM D256 standard), while the tensile testing samples were injection molded as dumbbell shaped specimens with dimensions of 160 mm long x 13 mm wide (at the neck) x 3 mm thick (ISO 527 standard).

2.3 UV- and heat-exposure conditions

The thermal ageing of the tensile- and impact testing samples was done in an air circulating oven at 100 °C, with sampling times of 1, 2, 3, 4, 6, 8, 10 and 12 months.

The artificially simulated (accelerated) weathering was carried out in a QUV-se machine equipped with solar eye irradiance control and a UV-A lamp. The testing programme was set according to the ISO 4892-3 standard, and the conditions were chosen in accordance with Qatar's climatic conditions. The samples were exposed to

repetitive cycles of UV exposure and condensation. UV radiation was set for 8 hours with an irradiance level of 0.76 W m^{-2} at a wavelength of 340 nm. The maximum temperature used was 60 °C and the condensation was applied for 4 hours at a temperature of 50 °C. Samples were collected after 0, 1000, 1500 and 2000 hours for both LDPE-A and LDPE-T. All the samples were turned around after each 250 h to ensure equal UV exposure on both sample sides.

2.4 Sample characterization

The molar mass distributions (MMD) of the samples were determined by HT-SEC. The measurements were realized with a PL 220 high-temperature size exclusion chromatograph (Polymer Laboratories, Church Stretton, UK). The temperature of the autosampler and the column compartment was set to 150 °C. A mobile phase flow rate of 1 mL/min was used. The polymer samples were dissolved for 4 h in TCB (containing 1 g/L butylated hydroxytoluene as stabilizer) at 160 °C. A sample concentration of 2 g/L was used. 200 µL of polymer solution were injected per analysis. Each sample was analyzed twice and results were averaged. A guard column (PLgel Olexis, 50 x 7.5 mm (L x I.D.)) and three analytical columns (3 x PLgel Olexis, 300 x 7.5 mm (L x I.D.), with particle size 13 µm, Agilent, Waldbronn, Germany)) were used for separation. An infrared detector (IR4, PolymerChar, Valencia, Spain) was used for detection. Data were collected and processed using WinGPC-software (version 7) from PSS (Mainz, Germany). Molar masses were calibrated with polystyrene (PS) standards (Polymer Standards Services, PSS, Mainz, Germany).

Scanning electron microscopy (SEM) was performed on the surfaces of the dumbbell specimens, before and after tensile testing, in an FEI Quanta 200 electron microscope (Thermo Fischer Scientific, Hillsboro, USA) at an accelerating voltage of 2–5 kV. The samples were sputter gold coated for 30 s using an Agar sputter coater.

Fourier transform infrared (FTIR) spectra were obtained at room temperature using a PerkinElmer Frontier Spectrum 400 FTIR spectrometer connected to a MIRACLE ATR detector with a ZnSe crystal. Sixteen scans in the range of 4000-550 cm^{-1} were done on each sample. The carbonyl index (CI) was calculated using Equation 1 [20].

$$\mathrm{CI} = \frac{\text{Absorption of carbonyl species}_{\,1650-1800\ \mathrm{cm}^{-1}}}{\text{Absorption of C}-\text{H peak}_{\,1420-1480\ \mathrm{cm}^{-1}}} \quad (1)$$

Non-isothermal crystallization analysis was performed in a Perkin Elmer DSC8500 differential scanning calorimeter under nitrogen atmosphere. Samples (5–10 mg) were sealed in aluminum sample pans and were initially heated from 30 to 180 °C at 20 °C min^{-1} (1st heating), cooled to 30 °C at the same rate, and re-heated to 180 °C at the same rate (2nd heating). The melting enthalpy (ΔH_m) and peak temperature of melting (T_m) were obtained from the melting peaks in the first and second heating curves, while the crystallization temperature (T_c) and the crystallization enthalpy (ΔH_c) were obtained from the crystallization peak in the cooling curve.

Thermal decomposition was studied *via* thermogravimetric analysis in a PerkinElmer TGA-4000 TGA/DSC instrument. Approximately 5-10 mg of sample was heated from 30 to 600 °C at a heating rate of 20 °C min^{-1} under nitrogen atmosphere. The onset of decomposition temperature was defined as the temperature at 5% weight loss ($T_{d,5\%}$) and the temperature at the maximum rate of decomposition (T_d) was the temperature at the maximum of the peak in the derivative TGA curve.

The tensile properties were measured using a 'Lloyd LR50K plus' universal tester according to the ISO 527 standard where no pre-load was applied to the sample. An

elongation speed of 10 mm min^{-1} and a gauge length of 50 mm were used. The Young's modulus (E) was manually calculated from the slope of the stress-strain curve between strain values of 0.2 and 2.2%. A minimum of five specimens were tested for each sample. The impact properties of the samples were investigated using an Instron Wolpert PW5 impact tester according to ASTM D256. Specimens with dimensions of 63.5 mm x 12.7 mm x 3 mm were notched at the center (45° notch and 2 mm depth). The Izod impact strength (in kJ m^{-2}) was calculated according to Equation 2 [21].

$$a_{iN} = \frac{E_c}{h \text{ x } b_N} \qquad (2)$$

where E_c is the corrected measured absorbed energy during impact in J, h is the thickness of the tested specimen in mm, and b_N is the remaining width of the tested specimen in mm.

Chapter 3: Results and Discussion

3.1 Microscopic analysis

The surface morphology of the neat and stabilized samples before and after UV exposure was studied through SEM analysis. The samples were examined before and after tensile testing to investigate the effect of tensile forces on the developed cracks under UV exposure. All the SEM micrographs of LDPE-A and LDPE-T samples are presented in Figures 3 and 4. A significant degradation with many cracks was observed for both the neat LDPE-A and LDPE-T after 2000h exposure (Figure 3(c,d) and Figure 4(b,c)).

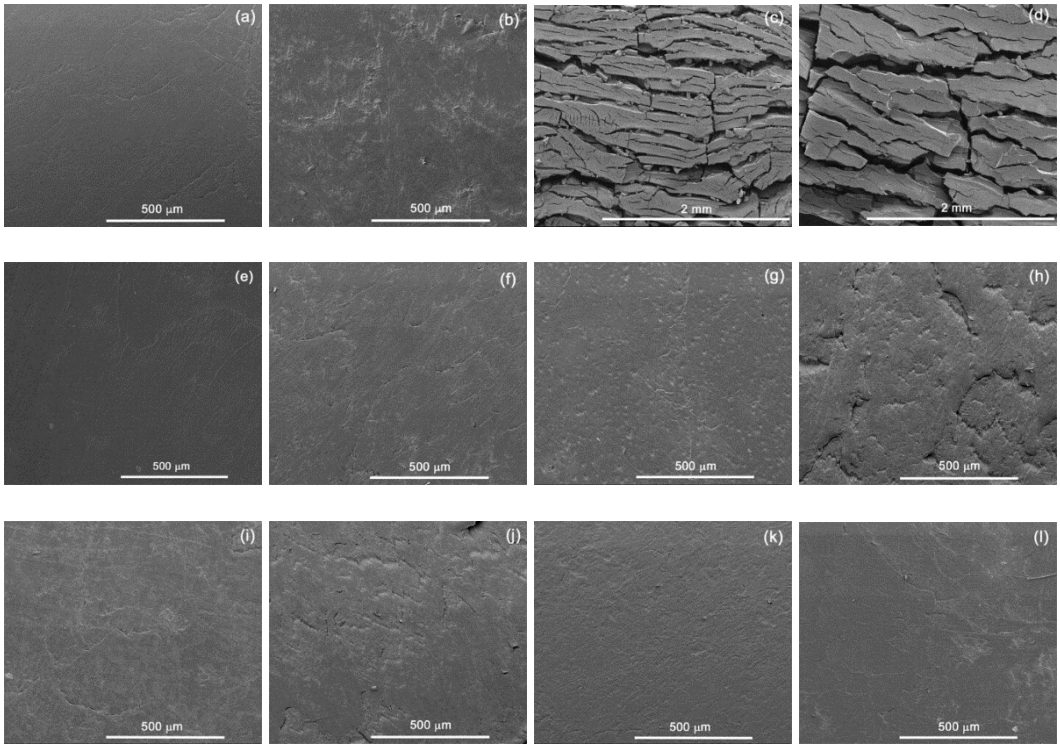

Figure 3. SEM images of: neat LDPE-A unexposed (a) and 2000 h exposed (c) before tensile testing, as well as unexposed (b) and 2000 h exposed (d) after tensile testing; LDPE-A/UV3 unexposed (e) and 2000 h exposed (g) before tensile testing, as well as unexposed (f) and 2000 h exposed (h) after tensile testing; LDPE-A/UV8 unexposed (i) and 2000 h exposed (k) before tensile testing, as well as unexposed (j) and 2000 h exposed (l) after tensile testing.

The crack size increased for both polymers after tensile testing, but not significantly. The most probable reason is that the cracks did not penetrate deep enough into the relatively thick sample during the duration of the UV exposure, and that the non-degraded part of the samples below the cracks to some extent maintained the sample integrity. The situation was very different for all the stabilized samples, where

much better surface integrity and almost no cracks was observed, even after long UV-exposure periods (Figure 2 (e)-(l) and Figure 3(d)-(k)). This is good indication that the additives were effective in protecting the samples from UV-initiated degradation.

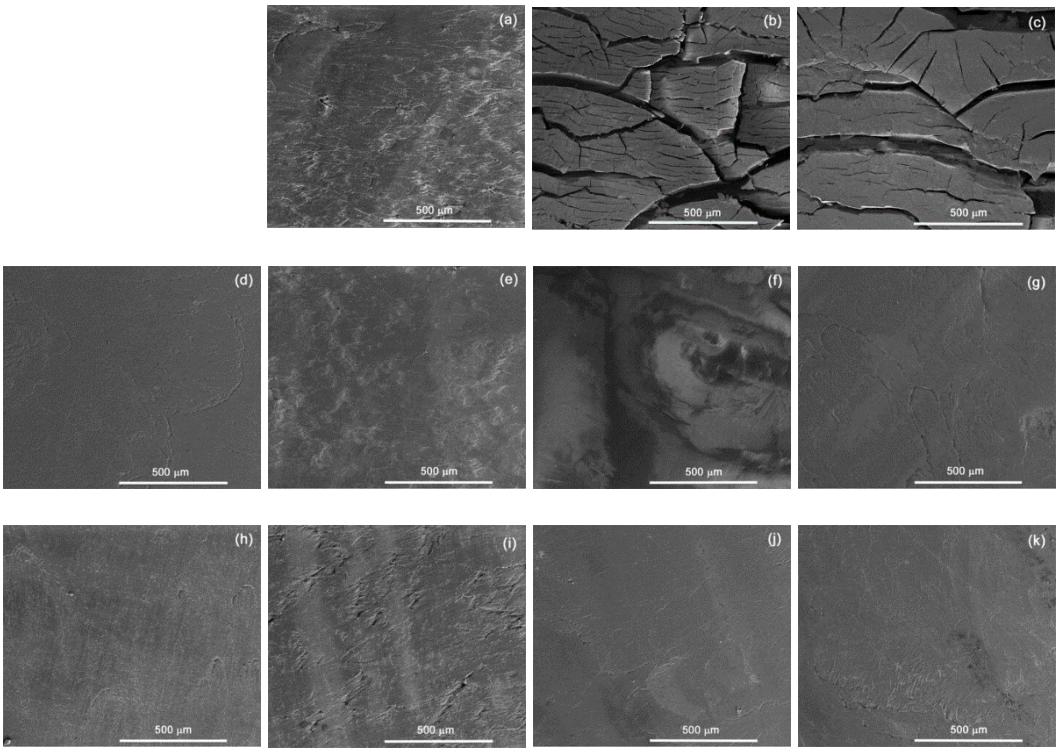

Figure 4. SEM images of: neat LDPE-T unexposed after tensile testing (a), as well as 2000 h exposed before (b) and after (c) tensile testing; LDPE-T/UV3 unexposed (d) and 2000 h exposed (f) before tensile testing, as well as unexposed (e) and 2000 h exposed (g) after tensile testing; LDPE-T/UV8 unexposed (h) and 2000 h exposed (j) before tensile testing, as well as unexposed (i) and 2000 h exposed (k) after tensile testing.

3.2 Molecular weight determination

Gel permeation chromatography (GPC) was used to observe changes in the molecular weight (MW) and MW distribution of the investigated samples as function of UV exposure time. A summary of the GPC results is shown in Tables 2 and 3. For the neat LDPE-A and LDPE-T, a significant decrease in average molecular weight was observed after the first 1000 h of UV exposure, followed by a slight further decrease after longer UV exposure periods. One would have expected a more significant reduction in molecular weight for neat LDPE-A than for neat LDPE-T, because LDPE-A has more tertiary carbons that are unstable and where chain scission can occur more easily, but it seems as if the UV exposure conditions were harsh enough for the two polymers to degrade at similar rates. It is further clear from Tables 4.3.1 and 4.3.2 that the molecular weight changed little for the stabilized samples of both polymers, confirming the effectiveness of both the UV3 and UV8 formulations.

Table 2. Results from the GPC analyses of all the investigated LDPE-A samples.

Sample	M_n / g mol^{-1}	M_w / g mol^{-1}	D
Neat LDPE-A (unexposed)	29764 ± 2441	345085 ± 4137	12 ± 1
LDPE-A/UV3 (unexposed)	27062 ± 3886	447215 ± 20131	17 ± 2
LDPE-A/UV8 (unexposed)	32238 ± 1505	441985 ± 14347	14 ± 1
Neat LDPE-A (1000 h UV exposed)	1436 ± 78	38325 ± 495	27 ± 2
LDPE-A/UV3 (1000 h UV exposed)	22281 ± 1271	405020 ± 12629	18 ± 1
LDPE-A/UV8 (1000 h UV exposed)	30921 ± 1718	427635 ± 7884	14 ± 1
Neat LDPE-A (1500 h UV exposed)	493 ± 127	50983 ± 34044	98 ± 44
LDPE-A/UV3 (1500 h UV exposed)	23143 ± 922	373975 ± 5112	16 ± 0
LDPE-A/UV8 (1500 h UV exposed)	29799 ± 1547	437715 ± 827	15 ± 1
Neat LDPE-A (2000 h UV exposed)	922 ± 1016	32783 ± 17539	64 ± 51
LDPE-A/UV3 (2000 h UV exposed)	22562 ± 2122	314285 ± 19099	14 ± 1
LDPE-A/UV8 (2000 h UV exposed)	25970 ± 1462	416665 ± 4151	16 ± 1

Table 3. Results from the GPC analyses of all the investigated LDPE-T samples.

Sample	M_n / g mol^{-1}	M_w / g mol^{-1}	D
Neat LDPE-T (unexposed)	29715 ± 1093	312385 ± 7686	11 ± 0
LDPE-T/UV3 (unexposed)	33002 ± 674	297505 ± 4094	9 ± 0
LDPE-T/UV8 (unexposed)	28716 ± 689	293885 ± 5650	10 ± 0
Neat LDPE-T (1000 h UV exposed)	2205 ± 123	38275 ± 6430	18 ± 4
LDPE-T/UV3 (1000 h UV exposed)	34362 ± 5330	320915 ± 8973	10 ± 2
LDPE-T/UV8 (1000 h UV exposed)	30548 ± 127	296540 ± 1810	10 ± 0
Neat LDPE-T (1500 h UV exposed)	2961 ± 810	50404 ± 10625	17 ± 1
LDPE-T/UV3 (1500 h UV exposed)	28929 ± 2481	338735 ± 12990	12 ± 2
LDPE-T/UV8 (1500 h UV exposed)	32721 ± 2943	294390 ± 11158	9 ± 1
Neat LDPE-T (2000 h UV exposed)	466 ± 84	31552 ± 7403	70 ± 29
LDPE-T/UV3 (2000 h UV exposed)	27146 ± 1945	264855 ± 11533	10 ± 0
LDPE-T/UV8 (2000 h UV exposed)	31016 ± 1369	296510 ± 5671	10 ± 1

3.3 Mechanical properties

3.3.1 Tensile testing

Tensile testing and impact testing were conducted to investigate the impact of UV- ageing on the mechanical properties of the neat and UV stabilized LDPEs. Figure 5, as well as Tables S1 and S2 in the Supplementary Information, summarizes the tensile properties of all the investigated samples. For neat LDPE-T, the Young's modulus increased almost linearly with increasing UV exposure time, while for LDPE-T it increased significantly up to 1000 h UV exposure, after which it did not change significantly within experimental error (Figure 5(a)).

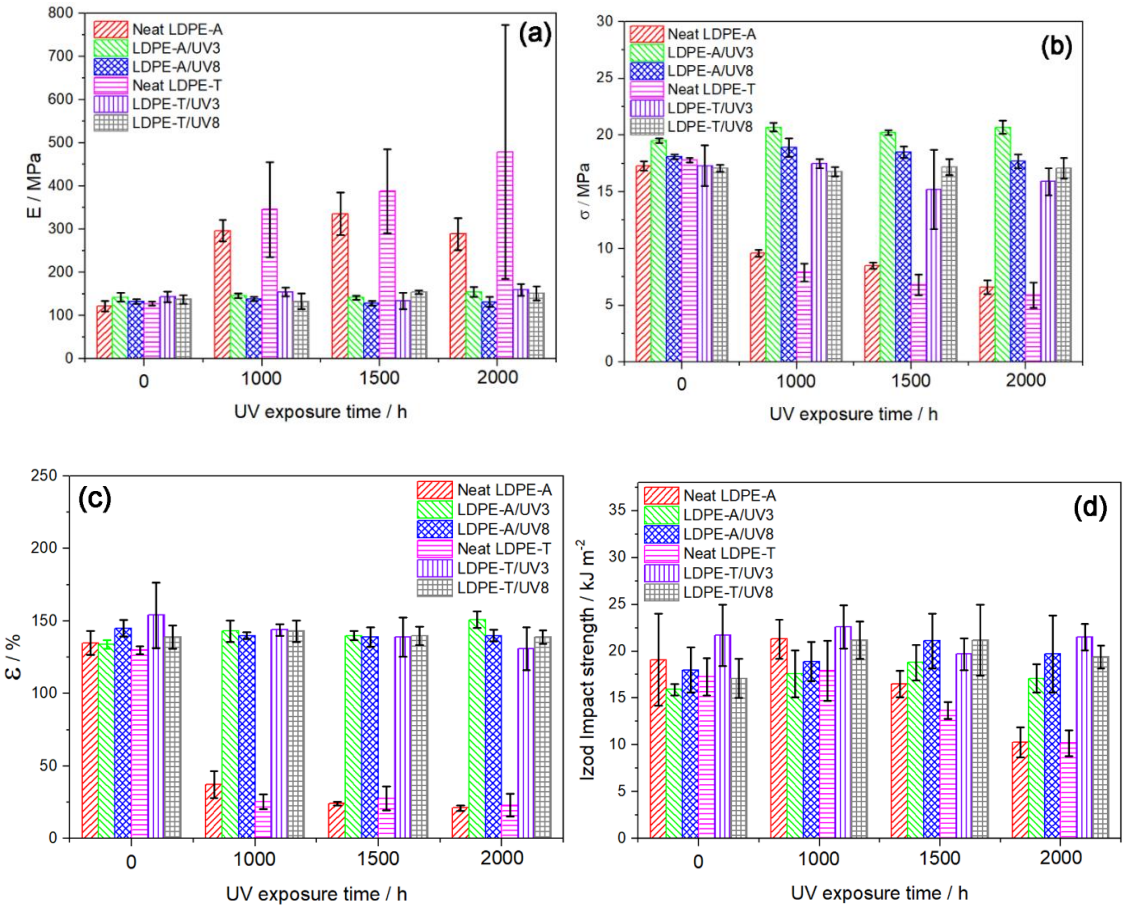

Figure 5. Comparison of the tensile and impact properties of LDPE-A, LDPE-T and their UV-protection formulations as function of UV exposure time.

These increasing modulus values are the result of the UV exposed samples being more crystalline, because UV initiated degradation will give rise to chain scission and the re-crystallization of the shorter chains. The LDPE-T samples further show much higher Young's modulus values than the LDPE-A samples, suggesting higher crystallinities for the LDPE-T samples.

However, the change in Young's modulus as a function of UV exposure time

for the stabilized samples of both polymers was negligible, and the values remained approximately the same with increasing UV exposure time. This is a strong indication that chain scission and re-crystallization into more crystalline polymers was absent during the UV exposure of these samples, which proves the effectiveness of the 'green' additives in protecting the LDPEs from UV initiated degradation.

The tensile strength and the strain at break for both neat LDPE-A and neat LDPE-T decreased significantly after 1000 h UV exposure, whereafter these values showed only slight further decreases with increasing UV exposure time (Figures 5(b,c)). This is to be expected because of the degradative chain scission taking place during UV exposure. It further seems as if there was very little difference between the two LDPEs regarding their tensile strength and strain at break values, which is in line with the observed changes in molecular weight.

There was almost no change in the tensile strength and strain at break of both the UV3 and UV8 stabilized LDPEs with increasing UV exposure time, and very little difference between the quantitative values of these two properties for the two different LDPEs. This is a further confirmation of the effectiveness of the formulations used to UV stabilize the LDPEs.

The tensile testing results of the heat exposed samples are summarized in Figure 6 and in Tables S3 and S4 in the Supplementary Information. All the LDPE-T compounds showed a higher modulus of elasticity (E) value, in the range of 180-242 MPa, while for LDPE-A the values ranged from 127 to 160 MPa. Lower strain at break (ε_{max}) values were recorded for LDPE-T, indicating a more brittle behaviour of the former. Finally, the tensile strength (σ_{max}) was determined in the range of 17-18 MPa, again slightly higher for the case of LDPE-T, but in accordance with literature [22]. The tensile results of the UV/heat stabilized compounds of LDPE-A (Figure 6, Table

S3 in Supplementary Information) indicate that for both LDPE-A/UV-3 and LDPE-A/UV-8 the values of σ_{max} and ε_{max} are very close to those of the neat LDPE-A, i.e. a variation of less than 7%. This should be expected since the loading level of the UV additives is very low, i.e. 0.2 wt%, therefore no significant variation in the mechanical behaviour is anticipated. However, it seems that the incorporation of the UV/heat additives resulted in a decrease in the *E* modulus values up to approximately 20%, rendering the particular materials more ductile. Regarding the tensile results of the UV/heat stabilized compounds of LDPE-T (Figure 6, Table S4 in Supplementary Information), it seems that for both LDPE-T/UV-3 and LDPE-T/UV-8 the values of σ_{max} are very close to those of neat LDPE-T, or within the error margin. However, the ε_{max} values are significantly higher, i.e. up to 35%, with a corresponding decrease in *E* modulus of up to 27%. Similarly, as in the case of LDPE-A, the incorporation of the UV/heat additives resulted in more ductile materials.

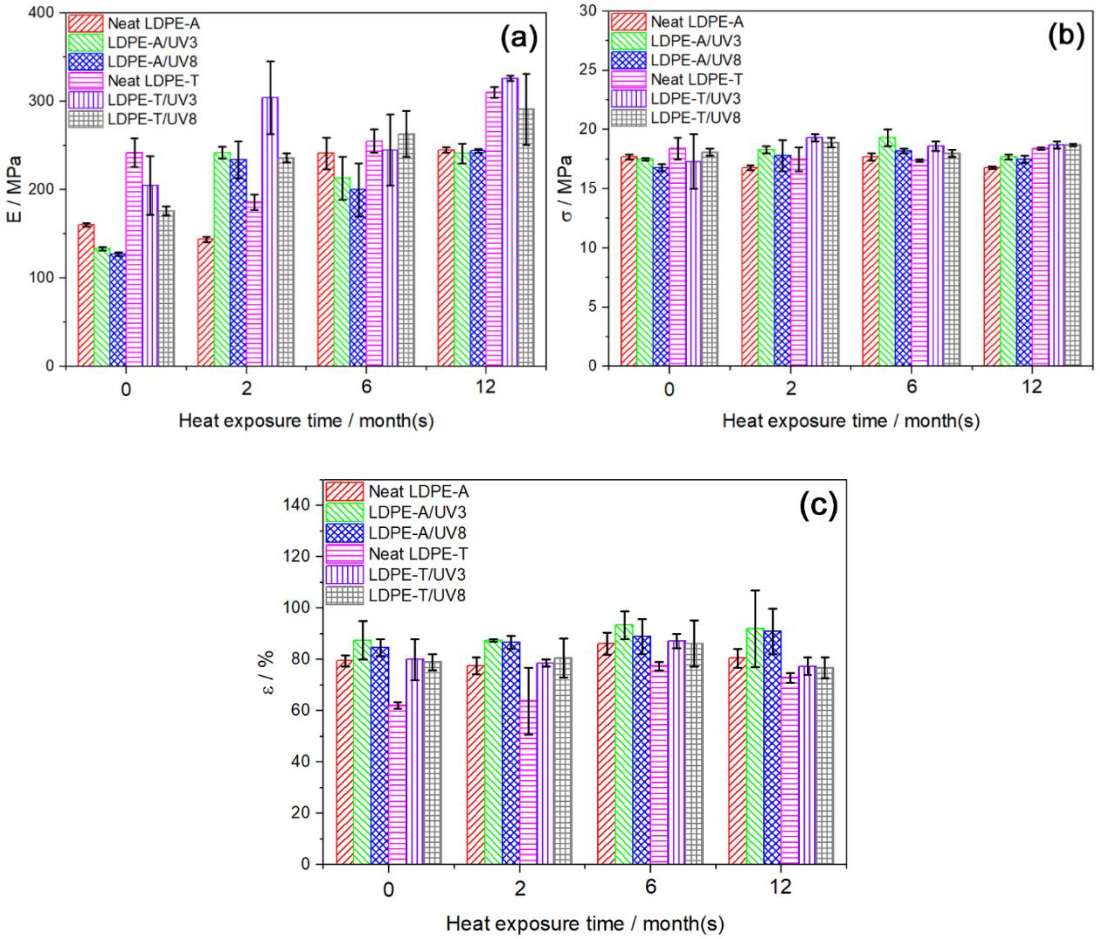

Figure 6. Comparison of the tensile properties of LDPE-A, LDPE-T and their UV/heat-protection formulations as function of heat exposure time.

For the oven-aged samples (1-12 months of exposure at 100 °C), neat LDPE-A and the respective UV/heat stabilized compounds show insignificant variations in the maximum strength and maximum strain values after ageing, with no clear trend. More specifically, σ_{max} was found to increase by 1.1 and 4.2% for LDPE-A/UV3 and LDPE-A/UV8, respectively from 0 to 12 months of exposure. On the other hand, ε_{max} was found decreased by 2.1% only for neat LDPE-A after 12 months of exposure. The

tensile strain values were found significantly increased by 24.3 and 18.8% for LDPE-A/UV3 and LDPE-A/UV8, respectively. The *E* modulus values after heat ageing increased, with the values from 0 to 12 months increasing by 81.8 and 91.8% for LDPE-A/UV3 and LDPE-A/UV8, respectively. This is an important observation, since it proves that all the materials became more brittle after ageing. All the LDPE-T and the respective UV/heat stabilized compounds showed a stabilized behaviour against heat in terms of maximum stress and strain. No clear trend was observed as in the case of LDPE-A. Once again, very low variations in maximum tensile stress were observed, except for LDPE-TR/UV3 where the σ_{max} increased by about 9% after 12 months. The tensile strain of neat LDPE-T d increased by 17.5%, while the UV/heat stabilized LDPE-T showed a decrease in tensile strain in the range of 2.8-6.9%. The *E* modulus of neat LDPE-T showed a significant decrease of about 26% after the initial 3 months of exposure, and then increased again to the final value of 310 MPa after 12 months of exposure (about 28% increase). For the rest of the UV/heat stabilized samples, the *E* modulus showed an increasing trend right from the first month of exposure, and the total increase after completion of the heat ageing was determined at 59.3 and 65.2% for LDPE-T/ UV3 and LDPE-T/UV8, respectively.

3.3.2 Impact testing

The impact strength for both LDPE-A and LDPE-T remained fairly constant up to 1000 h UV (Figure 5(d) and Table S5), but decreased fairly significantly up to 2000 h UV exposure. There was also little difference between the values for LDPE-A and LDPE-T. As with the other mechanical properties, there were no real changes in the impact strength of the stabilized samples for both polymers within experimental error. This again proves the effectiveness of the UV stabilization formulations.

3.4 Thermal analysis

3.4.1 Thermogravimetric analysis (TGA)

The thermal decomposition behaviour of the neat and UV-aged samples was investigated through TGA to determine their thermal stability. Figure 7 shows the TGA curves of all the samples, and the degradation temperatures are summarized in Table S6 in the Supplementary Information. All the samples showed a one-step decomposition.

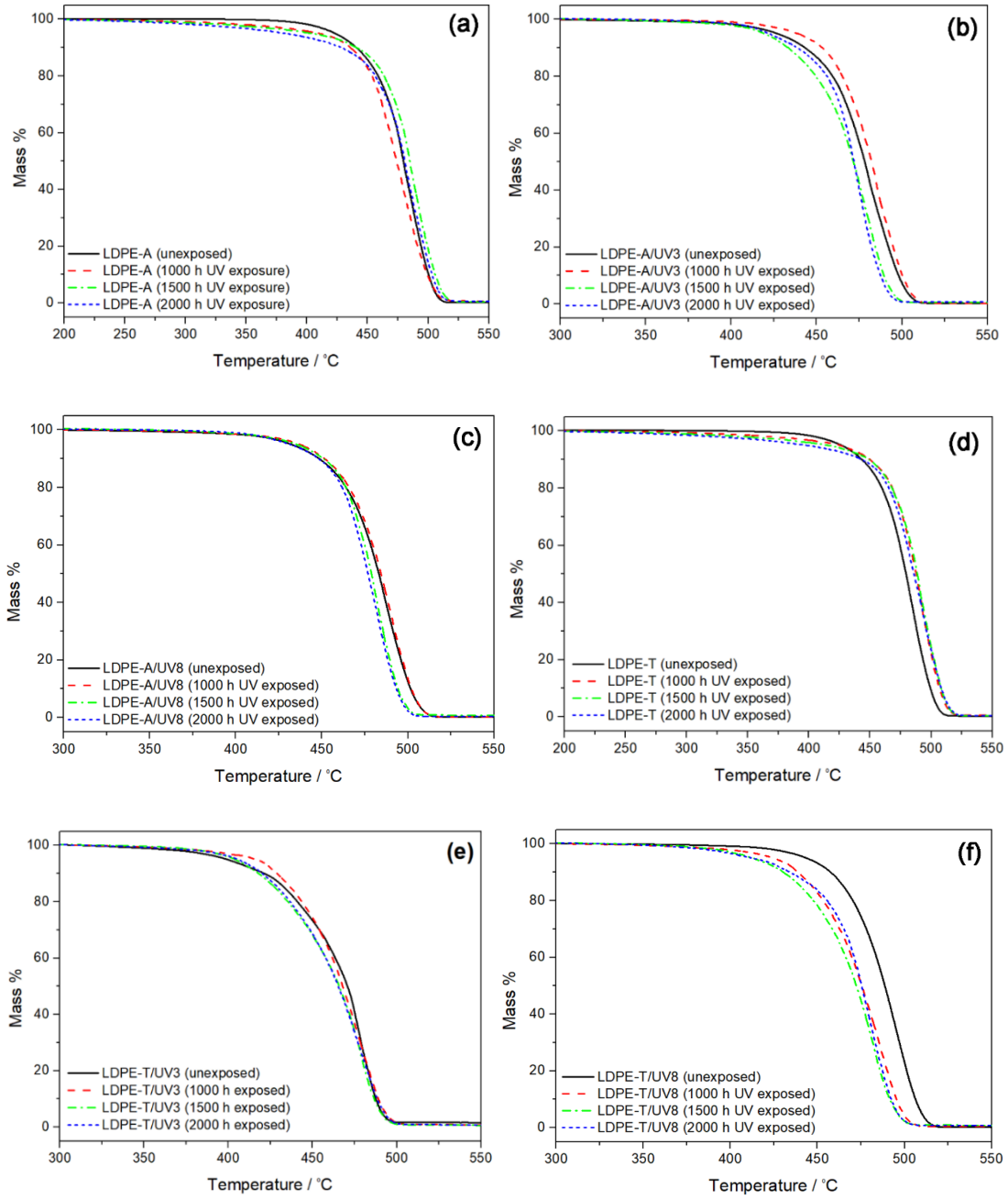

Figure 7. TGA curves in nitrogen atmosphere of (a) neat LDPE-A, (b) LDPE-A/UV3, (c) LDPE-A/UV8, (d) neat LDPE-T, (e) LDPE-T/UV3, and (f) LDPE-T/UV8 before and after UV exposure for different time periods.

For the unexposed polymers the maximum rate of mass loss was observed at 479 and 487 °C respectively for LDPE-A and LDPE-T, which indicates that LDPE-T is thermally more stable than LDPE-A. This can be attributed to the higher branching degree of LDPE-A, which causes this polymer to have more thermally unstable tertiary carbons. Similarly, the temperatures at maximum mass loss rate for the UV exposed neat samples showed higher values for LDPE-T in the range of 491 to 495 °C compared to those of LDPE-A, that are in the range of 472 to 482 °C. This indicates that LDPE-T is still thermally more stable than LDPE-A, even after long UV exposure times.

The unexposed UV3 and UV8 formulations of LDPE-A and LDPE-T generally showed better thermal stability than the neat polymers (Table S6). Among the four UV-stabilized formulations, LDPE-A/UV8 seems to be the best formulation in terms of thermal stability as it maintained a good stability even after long exposure periods. On the other hand, LDPE-T/UV8 was the least promising formulation in terms of thermal stability, because its thermal stability decreased significantly after only 1000 h of accelerated UV ageing (Figure 7(f)). Generally, the UV/heat stabilized LDPE-A samples were thermally more stable, and the thermal stability was less influenced by UV exposure than the stabilized LDPE-T samples, which is contrary to our observation for the neat polymers. This implies that the thermal stability of LDPE-A was enhanced more by the addition of the UV-stabilizers.

3.4.2 Differential scanning calorimetry (DSC)

DSC analyses were performed to follow the melting behaviour and crystallinity of the neat and UV/heat stabilized LDPEs. The DSC first heating and cooling curves of all the investigated samples are shown in Figure 8 and Figure S1. In this paper we shall discuss the first heating results for all the samples, because we are interested in

the initial influence of UV exposure on the melting behaviour and crystallinity of the different samples.

The melting temperatures of the main fractions of all the samples are very similar within experimental error. However, the melting enthalpies increased significantly after UV exposure for both the neat and stabilized samples (Tables S7 and S8). This indicates increased crystallinities as a result of degradative chain scission and re-crystallization of the neat samples, but it is not clear why increases in the enthalpies (crystallinities) were also observed for the UV3 and UV8 stabilized samples after accelerated UV exposure, because all the other results indicated very effective stabilization of the samples against UV initiated degradation. Generally, the differences between the corresponding enthalpies for the LDPE-A and LDPE-T based samples were within experimental error (Tables S7 and S8).

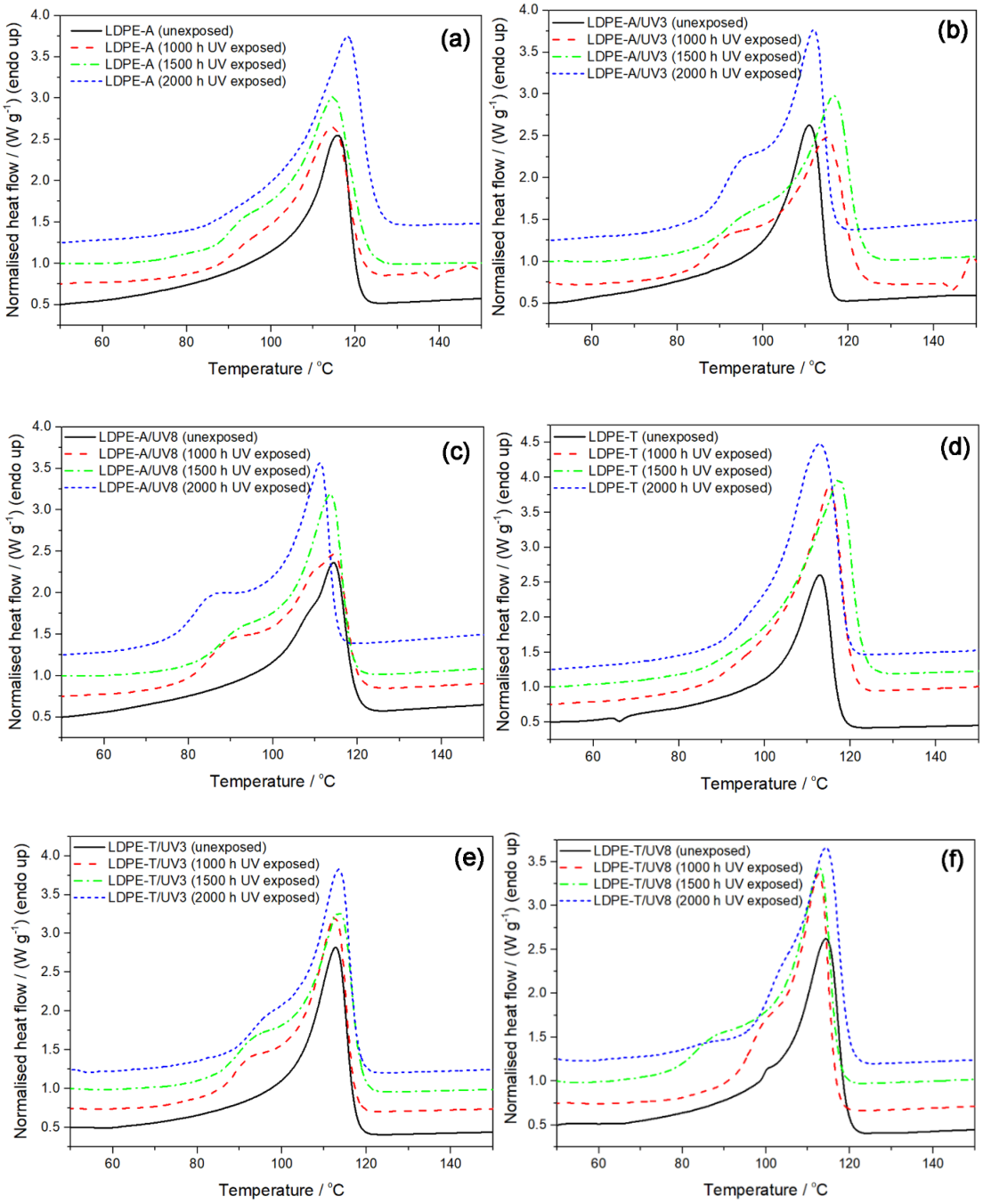

Figure 8. DSC first heating curves in nitrogen atmosphere of (a) neat LDPE-A, (b) LDPE-A/UV3, (c) LDPE-A/UV8, (d) neat LDPE-T, (e) LDPE-T/UV3, and (f) LDPE-T/UV8 before and after UV exposure for different time periods.

The first heating curves of the neat LDPEs showed a slight appearance of a lower temperature shoulder for the UV exposed samples, which was not observed for the unexposed samples. This could indicate the formation of a smaller crystal fraction as a result of UV initiated degradation and re-crystallization. For UV3 and UV8 stabilized samples of both LDPEs, the first heating curves all showed the development of a much more resolved lower temperature peak shoulder after accelerated UV exposure. This could be the result of the formation of smaller crystals around the UV stabilization additives, that acted as nucleation centres in both LLDPEs.

3.5 Fourier-transform infrared spectroscopy (FTIR)

FTIR analysis of all the samples were done in order to prove that oxidative degradation only occurred in the neat LDPE samples, and not in the UV3 and UV8 stabilized samples. Figure S2 clearly shows that there was no formation of carbonyl groups in the UV stabilized samples, while the neat LDPE-A and LDPE-T clearly show the formation of carbonyl groups on the LDPE chains after only 1000 h of accelerated UV exposure. The carbonyl indices reported in Table 4 are very similar for LDPE-A and LDPE-T, which indicates that the differences in polymer structure had little influence on the formation of carbonyl groups during the oxidative degradation process.

Table 4. Carbonyl index values of all the investigated samples before and after different periods of accelerated UV exposure.

Sample	Carbonyl index	Sample	Carbonyl index
LDPE-A (unexposed)	-	LDPE-T (unexposed)	-
LDPE-A/UV3 (unexposed)	-	LDPE-T/UV3 (unexposed)	-
LDPE-A/UV8 (unexposed)	-	LDPE-T/UV8 (unexposed)	-
LDPE-A (1000 h UV)	0.88	LDPE-T (1000 h UV)	0.85
LDPE-A/UV3 (1000 h UV)	-	LDPE-T/UV3 (1000 h UV)	-
LDPE-A/UV8 (1000 h UV)	-	LDPE-T/UV8 (1000 h UV)	-
LDPE-A (1500 h UV)	0.85	LDPE-T (1500 h UV)	0.79
LDPE-A/UV3 (1500 h UV)	-	LDPE-T/UV3 (1500 h UV)	-
LDPE-A/UV8 (1500 h UV)	-	LDPE-T/UV8 (1500 h UV)	-
LDPE-A (2000 h UV)	0.93	LDPE-T (2000 h UV)	0.87
LDPE-A/UV3 (2000 h UV)	-	LDPE-T/UV3 (2000 h UV)	-
LDPE-A/UV8 (2000 h UV)	-	LDPE-T/UV8 (2000 h UV)	-

Conclusions

The morphology, thermal and mechanical properties of two different UV/HALS stabilizer formulations incorporated in two different low-density polyethylene grades with different structures were investigated using SEM, GPC, DSC, TGA, FTIR, tensile and impact testing after exposing them to artificial UV/heat conditions through accelerated (artificial) weathering and thermal ageing tests. The SEM micrographs showed a significant degradation for neat LDPE-A and LDPE-T after 2000 h exposure, whereas almost no cracks were observed for all the stabilized samples. The GPC results confirmed the observed SEM morphologies where a significant decrease in average molecular weight was detected for the neat LDPEs, while only a little change was observed for the stabilized samples of the two polymers. GPC results also showed that LDPE-A is much more compact than LDPE-T. LDPE-T was found to have much higher Young's modulus values than LDPE-A. The TGA results for the neat polymers showed that LDPE-T is thermally more stable than LDPE-A, even after long UV exposure times. However, LDPE-A was thermally more stable than LDPE-T for the stabilized samples, which indicates that the addition of the UV-stabilizers more effectively enhanced the thermal stability of LDPE-A. The carbonyl indices for both LDPE-A and LDPE-T were very similar, which reveals that the differences in polymer structure had little influence on the formation of carbonyl groups during the oxidative degradation process. Generally, the UV stabilization formulations were effective in maintaining good mechanical and thermal properties for both polymers. The results of this study show clearly the efficiency of the selected UV absorbers in absorbing the harmful UV radiation, and they also prove that the used HALS additives were successful in trapping the radicals and slowing down the photo- and thermal degradation processes.

References

[1] P.M.M.Van Erdeghem, F. Logist, M. Vallerio, C. Dittrich, J.F. Van Impe. Model based optimisation of tubular reactors for LDPE production. 8th IFAC Symposium on Advanced Control of Chemical Processes. The International Federation of Automatic Control, Singapore, July 10-13, 2012, p.786-791.

[2] S. Ronca, Polyethylene, in M. Gilbert (Ed.), Brydson's Plastics Materials, 8th ed., Elsevier Ltd (Amsterdam), 2017, p.247–278.

[3] I. Grigoriadou, K.M. Paraskevopoulos, K. Chrissafis, E. Pavlidou, T.G. Stamkopoulos, D. Bikiaris. Effect of different nanoparticles on HDPE UV stability. Polymer Degradation and Stability 2011; 96:151-163.

[4] M. Lu, P. Liu, S. Zhang, W. Yuan, S. Ding, F. Wang, Y. Ding, M. Yang. Anti-aging behavior of amino-containing co-condensed nanosilica in polyethylene. Polymer Degradation and Stability 2018; 154:137-148.

[5] D. Feldman. Polymer weathering: Photo-oxidation. Journal of Polymers and the Environment 2002; 10:163–173.

[6] V. Ambrogi, C. Carfagna, P. Cerruti, and V. Marturano. Additives in Polymers, in C. Jasso-Gastinel, J. Kenny (Eds), Modification of Polymer Properties, 2017, p.87-108.

[7] N.C. Jacob, R. Dhib. Nonlinear MPC of a multi-zone multi-feed LDPE autoclave reactor. Journal of Industrial and Engineering Chemistry 2012; 18:1781-1795.

[8] G.C. Pandey, B.P. Singh, A.K. Kulshreshtha. Morphological characterization of autoclave and tubular LDPE by high temperature IR spectroscopy. Polymer Testing 1990; 9:341–351.

[9] A.S. Luyt, S.S. Malik, S.A. Gasmi, A. Porfyris, A. Andronopoulou, D. Korres, S. Vouyiouka, M. Grosshauser, R. Pfaendner, R. Brüll, C. Papaspyrides. Halogen-

free flame-retardant compounds. Thermal decomposition and flammability behavior for alternative polyethylene grades. Polymers 2019; 11:1479.

[10] R. Kuhn, H. Kromer. Structures and properties of different low density polyethylenes. Colloid and Polymer science 1982; 1092:1083-1092.

[11] A.A. Basfar, K.M. Idriss Ali. Natural weathering test for films of various formulations of low density polyethylene (LDPE) and linear low density polyethylene (LLDPE). Polymer Degradation and stability 2006; 91:437-443.

[12] S.M. Al-Salem. Influence of natural and accelerated weathering on various formulations of linear low density polyethylene (LLDPE) films. Materials and Design 2009; 30:1729-1736.

[13] M. Scoponi, S. Cimmino, M. Kaci. Photo-stabilisation mechanism under natural weathering and accelerated photo-oxidative conditions of LDPE films for agricultural applications. Polymer 2000; 41:7969-7980.

[14] K. Cristofoli, R.N. Brandalise, M. Zeni. Photostabilized LDPE films with UV absorber and HALS as protection against the light for rosé sparkling wine. Journal of Food Processing and Technology 2012; 3:7.

[15] P.P.N. Siqueira, V.H. Magalhães, S.L.G de Andrade. Behavior of linear low-density polyethylene films under UV ageing for agricultural application, in J.S. Carpenter, C. Bai, J.P. Escobedo, J.Y. Hwang, S. Ikhmayies, B. Li, J. Li, S.N. Monteiro, Z. Peng, M. Zhang (Eds.), Characterization of Minerals, Metals, and Materials 2015, p.253-258.

[16] G. Wypych, Handbook of UV Degradation and Stabilization. 2015.

[17] M. Edge, J.M. Peña, C.M. Liauw, B. Valange, N.S. Allen. Studies of synergism between carbon black and stabilisers in LDPE photodegradation. Polymer Degradation and Stability 2001; 72:259-270.

[18] P. Gijsman. A review on the mechanism of action and applicability of hindered amine stabilizers. Polymer Degradation and Stability 2017; 145:2-10.

[19] W.W. Focke, R.P. Mashele, N.S. Nhlapo. Stabilization of low-density polyethylene films containing metal stearates as photodegradants. Journal of Vinyl and Additives Technology 2011; 21:129-133.

[20] Y.C. Hsu, M.P. Weir, R.W. Truss, C.J. Garvey, T.M. Nicholson, P.J. Halley. A fundamental study on photo-oxidative degradation of linear low-density polyethylene films at embrittlement. Polymer 2012; 53:2385-2393.

[21] D.M. Simpson, G.A. Vaughan. Ethylene polymers, LLDPE. Encyclopedia of Polymer Science and Technology 2001; 2:441-482.

[22] N. Maraschin. Ethylene polymers LDPE. Encyclopedia of Polymer Science and Technology. NJ: Wiley & Sons.

Supplementary Information

Table S 1. Tensile testing results for all the investigated LDPE-A samples

Sample	E / MPa	σ / MPa	ε / %
Neat LDPE-A (unexposed)	122 ± 12	17.3 ± 0.4	135 ± 8
LDPE-A/UV3 (unexposed)	143 ± 10	19.5 ± 0.2	134 ± 3
LDPE-A/UV8 (unexposed)	133 ± 5	18.1 ± 0.2	145 ± 6
Neat LDPE-A (1000 h UV exposed)	297 ± 24	9.7 ± 0.3	37.3 ± 9.1
LDPE-A/UV3 (1000 h UV exposed)	146 ± 5	20.7 ± 0.4	143 ± 7
LDPE-A/UV8 (1000 h UV exposed)	139 ± 4	18.9 ± 0.8	140 ± 2
Neat LDPE-A (1500 h UV exposed)	336 ± 49	8.5 ± 0.3	24.1 ± 1.3
LDPE-A/UV3 (1500 h UV exposed)	142 ± 5	20.2 ± 0.2	140 ± 3
LDPE-A/UV8 (1500 h UV exposed)	129 ± 6	18.5 ± 0.5	139 ± 7
Neat LDPE-A (2000 h UV exposed)	289 ± 37	6.6 ± 0.7	21.1 ± 2.0
LDPE-A/UV3 (2000 h UV exposed)	155 ± 12	20.7 ± 0.6	151 ± 6
LDPE-A/UV8 (2000 h UV exposed)	132 ± 12	17.7 ± 0.6	140 ± 4

Table S 2. Tensile testing results for all the investigated LDPE-T samples

Sample	E / MPa	σ / MPa	ε / %
Neat LDPE-T (unexposed)	128 ± 5	17.8 ± 0.2	130 ± 3
LDPE-T/UV3 (unexposed)	144 ± 12	17.3 ± 1.8	154 ± 23
LDPE-T/UV8 (unexposed)	138 ± 10	17.1 ± 0.3	139 ± 8
Neat LDPE-T (1000 h UV exposed)	346 ± 110	7.9 ± 0.8	25.6 ± 5.0
LDPE-T/UV3 (1000 h UV exposed)	155 ± 10	17.5 ± 0.4	144 ± 4
LDPE-T/UV8 (1000 h UV exposed)	133 ± 18	16.8 ± 0.4	143 ± 7
Neat LDPE-T (1500 h UV exposed)	388 ± 97	6.9 ± 0.9	27.7 ± 8.2
LDPE-T/UV3 (1500 h UV exposed)	134 ± 19	15.2 ± 3.5	139 ± 13
LDPE-T/UV8 (1500 h UV exposed)	155 ± 4	17.2 ± 0.8	140 ± 6
Neat LDPE-T (2000 h UV exposed)	354 ± 102	5.9 ± 1.1	23.0 ± 7.8
LDPE-T/UV3 (2000 h UV exposed)	160 ± 14	15.9 ± 1.2	131 ± 15
LDPE-T/UV8 (2000 h UV exposed)	152 ± 16	17.1 ± 0.9	139 ± 5

Table S 3. Tensile testing results for all the investigated LDPE-A samples (heat exposure)

Sample	σ / MPa	ε / %	*E* / MPa
Neat LDPE-A (unexposed)	17.7 ± 0.2	82.2 ± 2.2	160 ± 2
LDPE-A/UV3 (unexposed)	17.5 ± 0.1	74.0 ± 3.4	133 ± 2
LDPE-A/UV8 (unexposed)	16.8 ± 0.3	76.6 ± 4.0	127 ± 2
Neat LDPE-A (1 month heat exposed)	16.6 ± 0.5	75.8 ± 3.7	158 ± 8
LDPE-A/UV3 (1 month heat exposed)	18.2 ± 0.4	80.4 ± 4.0	243 ± 13
LDPE-A/UV8 (1 month heat exposed)	17.5 ± 0.4	93.5 ± 8.3	226 ± 23
Neat LDPE-A (2 months heat exposed)	16.8 ± 0.2	77.6 ± 3.4	144 ± 3
LDPE-A/UV3 (2 months heat exposed)	18.3 ± 0.3	87.4 ± 0.5	242 ± 7
LDPE-A/UV8 (2 months heat exposed)	17.8 ± 1.3	86.6 ± 2.5	234 ± 21
Neat LDPE-A (3 months heat exposed)	16.4 ± 0.9	79.5 ± 2.2	148 ± 10
LDPE-A/UV3 (3 months heat exposed)	18.8 ± 0.3	87.5 ± 7.5	209 ± 9
LDPE-A/UV8 (3 months heat exposed)	19.0 ± 0.7	84.7 ± 3.3	202 ± 3
Neat LDPE-A (4 months heat exposed)	18.3 ± 0.4	82.1 ± 3.5	265 ± 38
LDPE-A/UV3 (4 months heat exposed)	18.0 ± 0.4	90.6 ± 4.8	237 ± 13
LDPE-A/UV8 (4 months heat exposed)	18.1 ± 0.3	93.6 ± 2.0	205 ± 27
Neat LDPE-A (6 months heat exposed)	17.7 ± 0.3	86.1 ± 4.3	241 ± 18
LDPE-A/UV3 (6 months heat exposed)	19.3 ± 0.7	93.4 ± 5.4	213 ± 24
LDPE-A/UV8 (6 months heat exposed)	18.2 ± 0.2	89.0 ± 6.8	200 ± 30
Neat LDPE-A (8 months heat exposed)	17.1 ± 2.1	91.1 ± 12.3	225 ± 12
LDPE-A/UV3 (8 months heat exposed)	18.1 ± 0.4	91.9 ± 6.1	223 ± 9
LDPE-A/UV8 (8 months heat exposed)	17.5 ± 0.3	94.4 ± 5.6	229 ± 8
Neat LDPE-A (10 months heat exposed)	17.7 ± 0.6	88.1 ± 8.3	236 ± 9
LDPE-A/UV3 (10 months heat exposed)	18.2 ± 0.6	93.2 ± 16.5	234 ± 5
LDPE-A/UV8 (10 months heat exposed)	17.4 ± 0.9	87.1 ± 2.3	233 ± 5
Neat LDPE-A (12 months heat exposed)	16.8 ± 0.1	80.5 ± 3.6	245 ± 3
LDPE-A/UV3 (12 months heat exposed)	17.7 ± 0.2	92.0 ± 15.0	241 ± 11
LDPE-A/UV8 (12 months heat exposed)	17.5 ± 0.3	91.0 ± 8.8	244 ± 2

Table S 4. Tensile testing results for all the investigated LDPE-T samples (heat exposure)

Sample	σ / MPa	ε / %	*E* / MPa
Neat LDPE-T (unexposed)	18.4 ± 0.9	62.1 ± 1.3	242 ± 16
LDPE-T/UV3 (unexposed)	17.3 ± 2.3	80.0 ± 8.0	205 ± 33
LDPE-T/UV8 (unexposed)	18.1 ± 0.3	79.0 ± 3.1	176 ± 5
Neat LDPE-T (1 month heat exposed)	17.7 ± 0.3	69.4 ± 4.2	183 ± 2
LDPE-T/UV3 (1 month heat exposed)	18.6 ± 1.7	79.8 ± 6.6	293 ± 36
LDPE-T/UV8 (1 month heat exposed)	18.7 ± 0.5	76.1 ± 5.2	303 ± 14
Neat LDPE-T (2 months heat exposed)	17.5 ± 1.0	63.8± 13.1	186 ± 9
LDPE-T/UV3 (2 months heat exposed)	19.3 ± 0.3	78.7 ± 1.4	304 ± 41
LDPE-T/UV8 (2 months heat exposed)	18.9 ± 0.4	80.5 ± 7.6	236 ± 5
Neat LDPE-T (3 months heat exposed)	17.6 ± 0.3	74.3 ± 1.5	178 ± 4
LDPE-T/UV3 (3 months heat exposed)	19.4 ± 0.3	80.2 ± 6.4	241 ± 12
LDPE-T/UV8 (3 months heat exposed)	18.0 ± 0.1	82.8 ± 2.7	263 ± 5
Neat LDPE-T (4 months heat exposed)	17.3 ± 0.1	78.3 ± 3.2	255 ± 8
LDPE-T/UV3 (4 months heat exposed)	19.1 ± 1.0	86.4 ± 5.3	253 ± 42
LDPE-T/UV8 (4 months heat exposed)	18.2 ± 0.5	81.0 ± 5.8	215 ± 42
Neat LDPE-T (6 months heat exposed)	17.4 ± 0.1	77.5 ± 1.7	255 ± 13
LDPE-T/UV3 (6 months heat exposed)	18.6 ± 0.4	87.2 ± 2.8	245 ± 40
LDPE-T/UV8 (6 months heat exposed)	18,0 ± 0.3	86.3 ± 9.1	263 ± 26
Neat LDPE-T (10 months heat exposed)	18.5 ± 0.2	63.5 ± 5.0	314 ± 8
LDPE-T/UV3 (10 months heat exposed)	19.3 ± 0.4	73.4 ± 2.4	309 ± 12
LDPE-T/UV8 (10 months heat exposed)	18.9 ± 0.2	77.2 ± 3.9	295 ± 20
Neat LDPE-T (12 months heat exposed)	18.4 ± 0.1	72.9 ± 2.0	310 ± 6
LDPE-T/UV3 (12 months heat exposed)	18.7 ± 0.3	77.4 ± 3.4	326 ± 3
LDPE-T/UV8 (12 months heat exposed)	18.7 ± 0.1	76.8 ± 4.1	291 ± 40

Table S 5. Impact testing results for all the investigated LDPE-A and LDPE-T samples

Sample	Izod impact strength / kJ m^2	Sample	Izod impact strength / kJ m^2
Neat LDPE-A (unexposed)	19.1 ± 4.9	Neat LDPE-T (unexposed)	17.3 ± 2.0
LDPE-A/UV3 (unexposed)	15.9 ± 0.6	LDPE-T/UV3 (unexposed)	21.7 ± 3.3
LDPE-A/UV8 (unexposed)	19.0 ± 2.4	LDPE-T/UV8 (unexposed)	17.1 ± 2.1
Neat LDPE-A (1000 h UV exposed)	21.3 ± 2.1	Neat LDPE-T (1000 h UV exposed)	17.9 ± 3.2
LDPE-A/UV3 (1000 h UV exposed)	17.6 ± 2.5	LDPE-T/UV3 (1000 h UV exposed)	22.6 ± 2.3
LDPE-A/UV8 (1000 h UV exposed)	18.9 ± 2.1	LDPE-T/UV8 (1000 h UV exposed)	21.2 ± 2.0
Neat LDPE-A (1500 h UV exposed)	16.5 ± 1.4	Neat LDPE-T (1500 h UV exposed)	13.7 ± 0.9
LDPE-A/UV3 (1500 h UV exposed)	18.8 ± 1.9	LDPE-T/UV3 (1500 h UV exposed)	19.7 ± 1.7
LDPE-A/UV8 (1500 h UV exposed)	21.1 ± 2.9	LDPE-T/UV8 (1500 h UV exposed)	21.2 ± 3.8
Neat LDPE-A (2000 h UV exposed)	10.3 ± 1.6	Neat LDPE-T (2000 h UV exposed)	10.2 ± 1.4
LDPE-A/UV3 (2000 h UV exposed)	17.1 ± 1.5	LDPE-T/UV3 (2000 h UV exposed)	21.5 ± 1.4
LDPE-A/UV8 (2000 h UV exposed)	19.7 ± 4.1	LDPE-T/UV8 (2000 h UV exposed)	19.4 ± 1.2

Table S 6. TGA onset of mass loss (Td,5%) and maximum mass loss rate (Td,max) temperatures for all the investigated samples.

LDPE-A	$T_{d,5\%}$ / °C	$T_{d,max}$/ °C	LDPE-T	$T_{d,5\%}$ / °C	$T_{d,max}$/ °C
Neat (unexposed)	422.8	478.7	Neat (unexposed)	426.2	487.0
UV3 (unexposed)	426.7	480.1	UV3 (unexposed)	399.0	477.1
UV8 (unexposed)	432.0	486.2	UV8 (unexposed)	443.4	495.6
Neat (1000 h UV)	409.0	472.0	Neat (1000 h UV)	424.7	490.9
UV3 (1000 h UV)	438.7	484.7	UV3 (1000 h UV)	416.5	480.4
UV8 (1000 h UV)	436.9	490.5	UV8 (1000 h UV)	424.7	487.4
Neat (1500 h UV)	403.4	485.6	Neat (1500 h UV)	414.6	490.4
UV3 (1500 h UV)	419.5	480.2	UV3 (1500 h UV)	403.8	478.9
UV8 (1500 h UV)	435.4	480.6	UV8 (1500 h UV)	412.4	482.3
Neat (2000 h UV)	381.0	482.6	Neat (2000 h UV)	396.9	495.3
UV3 (2000 h UV)	421.9	473.8	UV3 (2000 h UV)	405.8	480.4

Table S 7. DSC melting and crystallization temperatures and enthalpies of LDPE-A and its UV/heat stabilization formulations after different times of UV exposure.

Sample	First heating		Cooling		Second heating	
	T_m / °C	ΔH_m / J g^{-1}	T_c / °C	ΔH_c / Jg^{-1}	T_m / °C	ΔH_m / Jg^{-1}
Neat (unexposed)	116.6	62.6	95.8	-78.1	113.3	67.0
UV3 (unexposed)	111.1	60.0	94.3	-70.2	111.1	55.9
UV8 (unexposed)	115.7	60.6	92.8	-74.5	112.6	58.2
Neat (1000 h UV)	114.8	87.6	90.0	-72.7	113.1	50.8
UV3 (1000 h UV)	115.2	89.9	92.7	-71.8	113.9	59.5
UV8 (1000 h UV)	114.4	92.6	92.4	-73.9	113.5	52.6
Neat (1500 h UV)	114.8	107.4	89.6	-76.2	113.8	59.4
UV3 (1500 h UV)	116.8	90.1	92.7	-71.8	115.1	56.0
UV8 (1500 h UV)	113.8	86.0	93.1	-74.3	112.2	56.9
Neat (2000 h UV)	118.4	108.1	90.7	-81.6	115.7	66.9
UV3 (2000 h UV)	112.1	101.5	94.1	-73.2	111.2	65.7
UV8 (2000 h UV)	111.3	97.4	94.4	-71.3	110.5	52.7

Table S 8. DSC melting and crystallization temperatures and enthalpies of LDPE-T and its UV/heat stabilization formulations after different times of UV exposure.

Sample	First heating		Cooling		Second heating	
	T_m / °C	ΔH_m / J g^{-1}	T_c / °C	ΔH_c /Jg^{-1}	T_m / °C	ΔH_m / Jg^{-1}
Neat (unexposed)	111.3	60.1	94.0	-78.9	113.0	59.6
UV3 (unexposed)	113.1	65.6	94.6	-78.6	112.5	59.0
UV8 (unexposed)	113.8	69.6	94.1	-78.0	113.5	64.5
Neat (1000 h UV)	115.4	110.6	91.5	-86.2	112.6	69.1
UV3 (1000 h UV)	112.9	93.2	94.6	-79.2	112.6	60.5
UV8 (1000 h UV)	112.8	96.2	94.7	-78.6	112.7	60.1
Neat (1500 h UV)	117.7	115.2	93.0	-90.8	114.6	71.3
UV3 (1500 h UV)	113.8	99.9	93.7	-78.5	113.9	61.0
UV8 (1500 h UV)	113.0	92.6	94.6	-79.4	112.8	61.7
Neat (2000 h UV)	112.9	127.0	94.5	-97.4	111.7	80.4
UV3 (2000 h UV)	113.8	99.7	94.5	-78.4	113.7	62.7
UV8 (2000 h UV)	114.5	97.7	94.1	-78.1	114.0	60.8

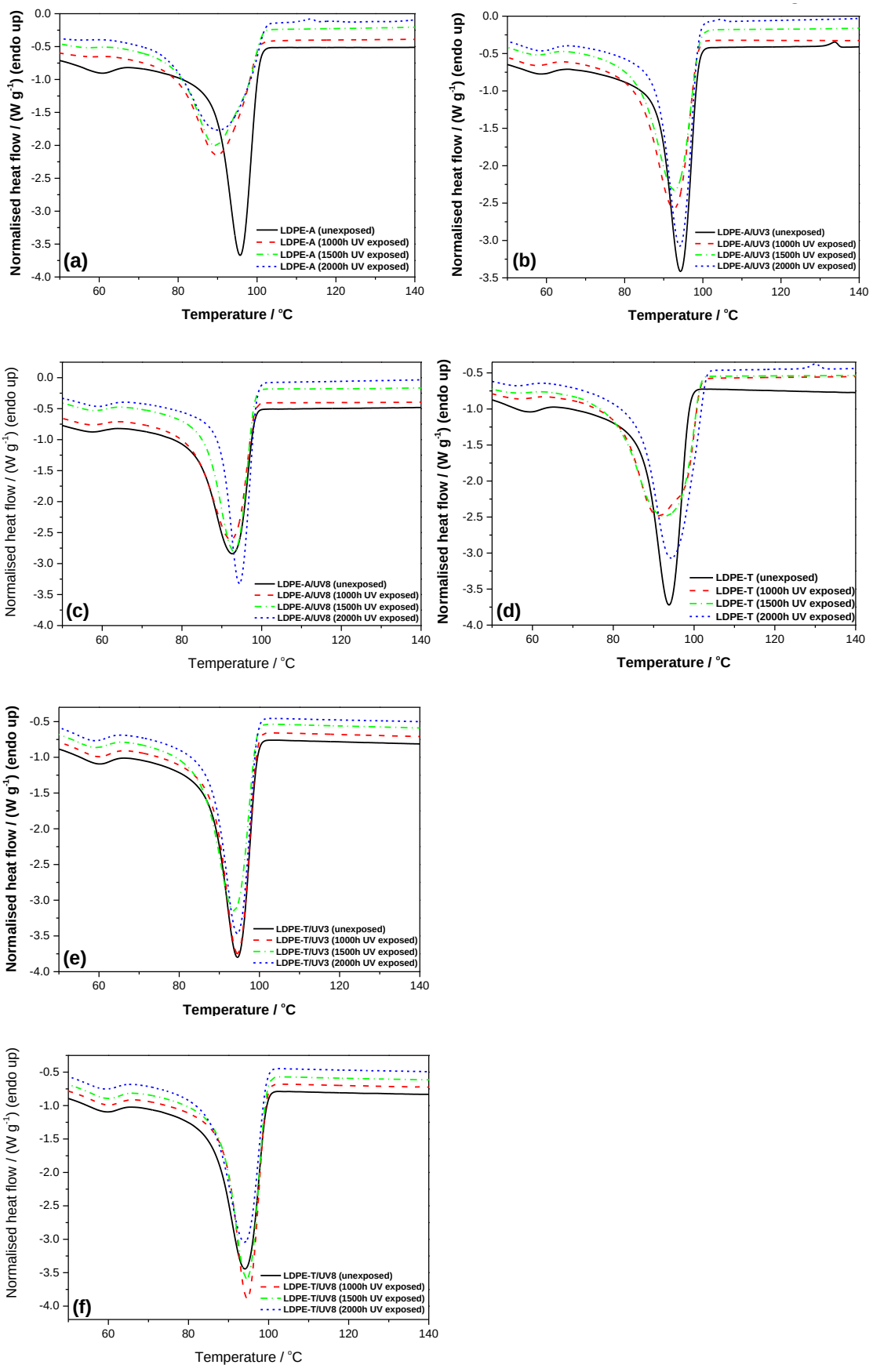

Figure S 1. DSC cooling curves in nitrogen atmosphere of (a) neat LDPE-A, (b) LDPE-

A/UV3, (c) LDPE-A/UV8, (d) neat LDPE-T, (e) LDPE-T/UV3, and (f) LDPE-T/UV8 before and after UV exposure for different time periods.

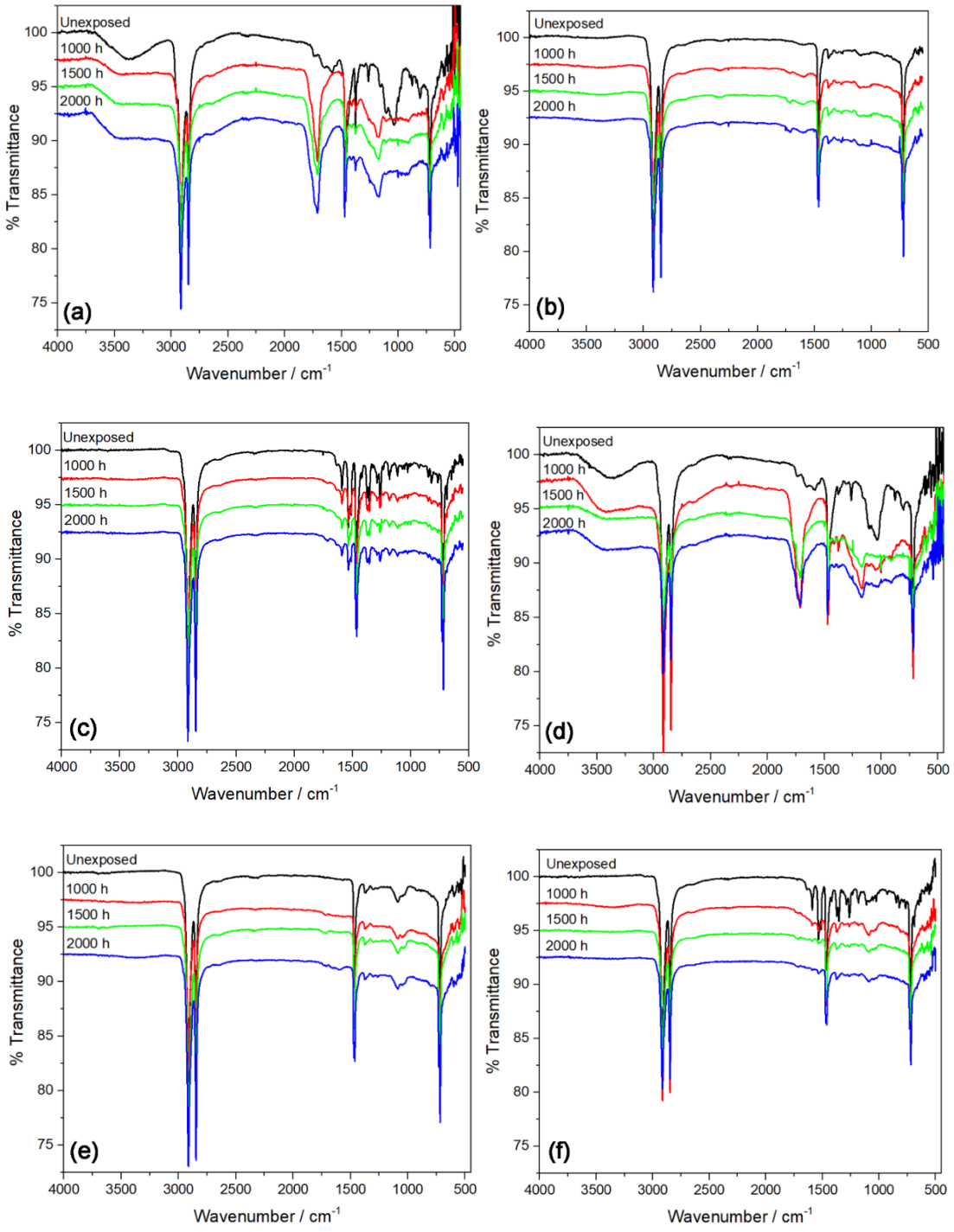

Figure S 2. FTIR spectra of (a) LDPE-A, (b) LDPE-A/UV3, (c) LDPE-A/UV8, (d) LDPE-T, (e) LDPE-T/UV3, and (f) LDPE-T/UV8 before UV exposure and after

different times of UV exposure. The peaks in these spectra were used for the calculation of the carbonyl index values in Table 3 of the paper.